Thermochimica Acta 492 (2009) 29–36

Contents lists available at ScienceDirect

Thermochimica Acta

journal homepage: www.elsevier.com/locate/tca

Thermal relaxation of water due to interfacial processes and phase equilibria in 1.8 nm pores of MCM-41

G.P. Johari*

Department of Materials Science and Engineering, McMaster University, 1280, Main Street West, Hamilton, Ontario, L8S 4L7, Canada

ARTICLE INFO

Article history:
Available online 10 March 2009

Keywords:
Water
MCM-41
Nanoconfinement
Enthalpy relaxation
Specific heat
Nucleation and growth
Ice

ABSTRACT

The available data on the enthalpy relaxation rate, dH_m/dt, and specific heat, $C_{p,m}$, of water in 1.8 nm pores of MCM-41 are interpreted by considering surface interactions and the number of H_2O molecules available to crystallize or vitrify. Out of a maximum of five H_2O molecules in a close-packing along the 1.8 nm diameter pore, at least two would form an uncrystallizable shell bonded to the silica wall and three would remain as a 1.1 nm diameter nanocore, which is too small for nucleation of the usual ice crystals. The dH_m/dt features observed in the temperature range of 90–130 K and 125–175 K show kinetic unfreezing or glass-softening characteristics. The first is attributed to the reorientation of H_2O in the nanoshell with little change in their center of mass position and the second to the change in the population of bonds between water and silica surface. The third dH_m/dt feature observed in the 180–230 K range is *inconsistent* with kinetic unfreezing or glass-softening and is attributed to the formation and melting of distorted ice-like unit cells with or without the growth- and stacking-faults that remain at equilibrium with the melt. The large increase in $C_{p,m}$ at T near 210 K is attributed to the latent heat of their "melting", as occurs on premelting of fine-grain ice and other solids. Data on the pore size dependence qualitatively support this interpretation. Structure of the water in nanopores depends on the pore size, and its properties differ from those of bulk water.

1. Introduction

A liquid in confinement is believed to supercool more easily than in the bulk state. The smaller is the confinement size the greater is the extent of supercooling. Part of this extent is real, and part of it is apparent because the freezing point itself is decreased in nanoconfinement. Nevertheless, the finding is seen as particularly useful in the current attempts to understand supercooled water's behavior in the bulk state [1–5] by assuming that configurational and vibrational properties of nanoconfined water are the same as those of the bulk. Two review articles [5,6] on the effects of nanoconfinement on melting and freezing have provided a list of various studies of water in large pores. Some of the calorimetric studies have been summarized by Schreiber et al. [7], Morishige and Kawano [8] and Tombari et al. [9]. Briefly, nanoconfined water has been studied by differential scanning calorimetry (DSC) [7,10–16], by modulated calorimetry [9,17], by isothermal [18] and by adiabatic calorimetry [2,19,20], mainly for the purpose of determining its configurational thermodynamics and freezing/melting behavior. Its dielectric spectra [21,22] have been studied for determining the relaxation times, and its Fourier transform spectra for understanding the vibrational features [1,15]. The majority of studies have been performed by using X-ray and neutron scattering for the purpose of identifying crystalline forms, the growth- and stacking-faults or other low entropy phases that may form on cooling and in some cases for determining the self-diffusion time of H_2O [5,13,14,23–39]. Orientational and other correlation times and freezing/melting features have also been studied extensively by NMR [4,13,16,40–47]. Such studies have been performed on water confined to pores of different size and distribution in silica gels, porous glass and Vycor, and in various size cylindrical pores of MCM-41 [48].

It is known that on cooling from 273 K, only part of the confined water crystallizes in pores larger than ~2.1–2.8 nm diameter [14–16]; in pores of smaller diameter, it does not apparently crystallize. When the pore size is typically ~3 nm diameter, water freezes to cubic ice, not to the lower energy hexagonal ice, or freezes to a mixture of the two ices with a persistent disordered structure [23–29,32,34,37–39], thus indicating that crystals and melt *coexist*. In several cases, freezing has produced distorted or defective lattice structure of the ices [28,32,34,35]. More recently, it has been found that, (i) freezing and melting in large nanopores occur over a wide temperature range with much less in MCM-41 than in Vycor [8,9,15,16,19,20], (ii) an ice–water equilibrium [15,29] persists over a certain temperature range, and (iii) C_p of water [17] and the

* Tel.: +1 905 525 9140; fax: +1 905 528 9295.
E-mail address: joharig@mcmaster.ca.

0040-6031/$ – see front matter © 2009 Elsevier B.V. All rights reserved.
doi:10.1016/j.tca.2009.02.021

energy of an H_2O molecule [18] vary with both its position in a nanopore and the amount of water [9,17,18] in the pore. It has also been recently shown [3] that the apparent peak in the molar specific heat, $C_{p,m}$, against the temperature plot for water confined to 1.1 nm pore of silica gel does not indicate the conjectured λ-type structural transition in nanoconfined or bulk water that may presumably change the activation energy for self-diffusion. It has been argued that relaxation studies of liquids in nanoconfinement would be useful for testing the configurational entropy's role in glass formation, because the activation energy for relaxation would become constant, as for an Arrhenius dynamics, after the cooperatively rearranging region of a supercooled liquid on cooling has grown to become equal to the pore size [49]. This would appear as a change from the Vogel–Fulcher–Tamman to Arrhenius behavior with change in the activation energy. In a review on supercooled water, Soper [26] has also discussed limitations of certain studies on nanoconfined water.

We focus on the features observed for water in 1.8 nm diameter cylindrical pores of MCM-41, and use Oguni et al.'s [2] data obtained from adiabatic calorimetry. They found that when a rapidly precooled sample of water confined to 1.8 nm pores was heated from 80 K, three exothermic peaks appeared in a plot of the molar heat release rate, $(-dH_m/dt)$, against the temperature T, and when the slowly precooled sample was similarly heated, three endothermic minima appeared in the $(-dH_m/dt)$ against T plots. These indicated three time scales at which kinetic unfreezing of the structure of nanopore water may have occurred. Also, when a precooled sample was heated, a remarkably large rise of $C_{p,m}$ to a sharp peak appeared in its plot against T. These findings led to reassigning of the glass-softening temperature T_g of nanoconfined and bulk water as ∼210 K [2], 74 K higher than 136 K, the T_g of bulk water measured for 30 K/min heating rate [50].

In particular, we consider the number of H_2O molecules that can fit across the diameter of a 1.8 nm pore, the possibility of nucleation of ice and phase equilibria, and the details of the time- and temperature-dependent $(-dH_m/dt)$ and $C_{p,m}$ features. This leads to the conclusion that the lowest temperature $(-dH_m/dt)$ feature arises from the kinetic unfreezing of orientational motion of H_2O in the uncrystallizable, one-molecule thick nanoshell bonded to the silica wall and the intermediate temperature feature arises from the breaking and reforming of the H_2O–silanol bond on the silica surface, both producing a glass-softening type feature on heating. The highest temperature $(-dH_m/dt)$ feature is *inconsistent* with kinetic unfreezing, and is attributed to a change in the equilibrium between the "melt-water" and the low entropy (and enthalpy), distorted ice-like structures and/or the growth- and stacking-faults in the remaining three-molecules thick nanocore. The unusually large $C_{p,m}$ rise is therefore due to the absorption of latent heat on T-dependent equilibrium "melting" of ice-like structures in a manner similar to that observed on equilibrium premelting of fine-grained ice and other solids. Available data on pore size dependence of these features qualitatively support the interpretation. The arguments provided here may be useful also in discussing the role of nanoconfined water in biological, geological, food and pharmaceutical sciences.

2. Enthalpy release and specific heat measurements of water in 1.8 nm pores

Since the method of adiabatic calorimetry for determining dH_m/dt and $C_{p,m}$ is not well known, we describe it briefly as in Oguni et al.'s study [2]. They determined $C_{p,m}$ by following the temperature of the sample for *ca.* 10 min after which the sample's temperature was taken as the initial value T_i. It was then heated at 0.1 K/min rate by supplying electrical energy, ΔE, and its temperature was followed again with time to determine the final temperature T_f. The difference, $(T_f - T_i)$, was used to determine, $C_{p,m} = \Delta E/(T_f - T_i)$. When the sample released or absorbed heat in its approach to equilibrium, a spontaneous temperature drift $(dT/dt)_{spont}$ occurred. The enthalpy release rate was determined from the relation, $(-dH_m/dt) = C_{p,m}(dT/dt)_{spont}$. T_g was empirically taken as the temperature at which the rapidly precooled sample showed a change from heat release to heat absorption, i.e., at $(-dH_m/dt) = 0$, and the slowly precooled sample showed a maximum of heat absorption rate, i.e., a minimum in the $(-dH_m/dt)$ plot against T. The characteristic relaxation time τ_0 at T_g was taken as ∼1 ks. The technique has been generally valuable for studying weak calorimetric effects of kinetic unfreezing of a disordered solid on heating and the resulting small $C_{p,m}$ rise. It has been especially valuable for detecting, (i) kinetic unfreezing of orientational motion of H_2O molecules in ice [51,52] and in ice clathrates [52–54] and their contribution to the entropy change, and (ii) the small $C_{p,m}$ rise from kinetic unfreezing of spectrally broad Johari–Goldstein (JG) relaxation [55,56] in glasses at T far below T_g.

For comparison, $C_{p,m}$ from a DSC experiment is determined by measuring the amount of heat transfer in Joules per second that is needed to raise (or lower) the temperature as the sample is heated (or cooled) at a rate q. Thus a DSC scan represents a plot which is equivalent to a plot of $qC_{p,m}$ against T. The integral of the DSC scan divided by q yields the enthalpy against T plot. When structural relaxation occurs during heating the plot shows a point of inflexion, which corresponds to the peak or minimum in $(-dH_m/dt)$ measured by adiabatic calorimetry. This has been illustrated by Oguni et al. in Fig. 1 of Refs. [2,20]. The rapidly precooled sample shows a point of inflexion corresponding to the exothermic peak in $(-dH_m/dt)$, and the slowly precooled sample shows on heating an endothermic minimum in $(-dH_m/dt)$. Although the adiabatic calorimetry and DSC techniques differ, the two probe the same equilibrium thermodynamic and relaxation effects, albeit on different time scales and in different manners.

It should be noted that in the packed, micron-size particles of water-containing MCM-41 (or silica gel powder), some of the water may form hydrogen bonds with the large surface of the particles and some may remain in the interparticle regions stabilized by the capillary forces. The excess water in the interparticle regions may freeze on cooling and the solid formed melt on heating [2]. Since the relative amounts of water in the pores and interparticle regions and on the surface vary with the total amount of water in MCM-41, the specific heat measured per gram of water vary, as does the profile of the $C_{p,app}$ against T plots. Water in nanopores is known to form a one-molecule thick layer attached by hydrogen bonds to the silica wall, thus producing a nanoshell of bonded water. It is also known as interfacial water. In partially filled pores, clusters of water attached to the nanoshell may exist. Experimentally, C_p in J/(g K) of pore water is determined by (a) subtracting the mass of dry silica powder from the sample's mass to estimate the total amount of water in the sample, (b) determining the mass of excess water (outside the pores) from the heat of fusion of ice determined from the melting peak area, (c) subtracting this mass from the total amount of water to obtain the mass of pore water, and finally, (d) subtracting the measured C_p in J/(g K) of the dry silica powder from the measured C_p of the sample per gram of pore water. Each of these steps adds to the error in the C_p reported for pore water, leading to a net error of at least ±2%.

The $(-dH_m/dt)$ data were read from the plots in Fig. 3 (bottom panel) from Oguni et al.'s paper [2] and are plotted against T here in Fig. 1. The sample precooled at 10 K/min to 80 K shows (dots) on heating three exotherms in $(-dH_m/dt)$. Among the two prominent exotherms, one appears in the 90–130 K range, and the other in the 180–230 K range with peaks at ∼108 K and 210 K. There is also a weak exotherm in the 130–170 K range with peak at ∼146 K. In

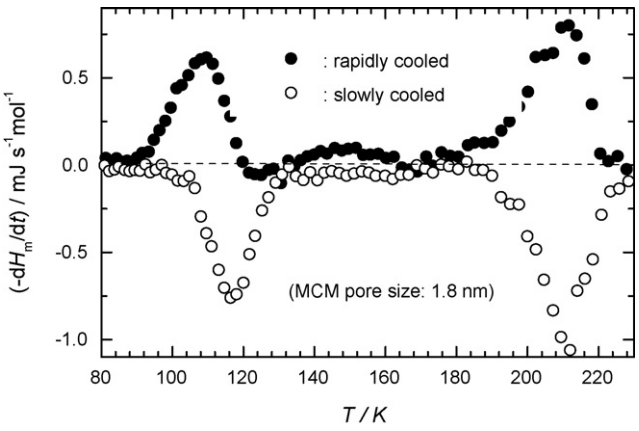

Fig. 1. Plots of the rate of enthalpy change against T measured at different temperatures when water in 1.8 nm pores of MCM-41 was heated after rapidly cooling to 80 K from ambient temperature and after slowly cooling to 80 K, as indicated. (Data are taken from Fig. 3 in Ref. [2].) Note that in the 90–130 K, and 128–170 K ranges, the exothermic $(-dH_m/dt)$ peak appears at a lower T than the endothermic $(-dH_m/dt)$ minimum, which meets the criteria for kinetic freezing or glass-softening. But in the 180–230 K range, the exothermic $(-dH_m/dt)$ peak and the endothermic $(-dH_m/dt)$ minimum appear at the same temperature, which does not meet this criterion.

contrast, the sample precooled at 15 mK/min (circles) to 80 K shows on heating two prominent endotherms in $(-dH_m/dt)$ in about the same T-range as the exotherms with minima at 117 K and 210 K, and a very weak endotherm in the 130–170 K range with a barely discernible minimum at ∼162 K.

The $C_{p,m}$ data were read from Fig. 2 in Ref. [2] and are plotted against T in Fig. 2 here. Oguni et al. [2] had reported also a small and broad, well-separated $C_{p,m}$ peak at ∼ 230 K, which they attributed to melting of bulk ice. They noted [2]: "About 5% of water crystallized within the 1.8 nm pores as estimated from the enthalpy of fusion." Because of its irrelevance for our analysis, this peak is not shown in Fig. 2.

3. Characteristic features of kinetic unfreezing

One of the premise for analysis here is the characteristic feature of $(-dH_m/dt)$ during the t- and T-dependent kinetic unfreezing of a disordered structure on heating, or during glass-softening. Here, we use only two such characteristics that are relevant to the $(-dH_m/dt)$ against T plots [2,20,51–54]:

(I) The exothermic peak on heating a rapidly precooled sample appears at a *lower* temperature than the endothermic minimum on heating the slowly precooled sample at the same rate.

(II) A weak endothermic minimum appears after the exothermic peak and a very small exothermic peak after the endothermic minimum.

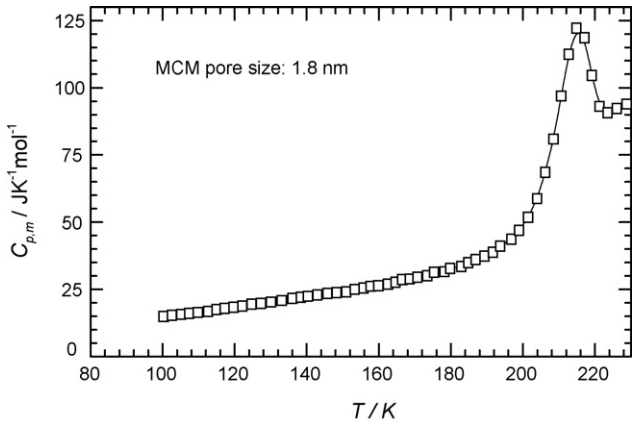

Fig. 2. Plot of the molar specific heat of water in 1.8 nm pores of MCM-41 against T. (Data taken from Fig. 2 in Ref. [2].)

Experiments on glasses and plastic crystals have shown feature I [2,20,51–54], and only high accuracy data have shown the very weak feature II.

Although our discussion is based on the features observed in the $(-dH_m/dt)$ against T plots, it is worth describing how those features appear in the usual description of the enthalpy against T plots constructed from a DSC scan. Briefly, features of $C_{p,m}$ and dH_m/dt against T plots on kinetic unfreezing are described by a non-exponential, nonlinear glass relaxation formalism developed by Tool [57], Narayanaswamy [58], and by Moynihan et al. [59],

$$\tau_0 = A\ \exp\left[\frac{x\Delta h^*}{RT} + \frac{(1-x)\Delta h^*}{RT_f}\right] \quad (1)$$

$$\phi = \phi_0\ \exp\left[-\left(\frac{t}{\tau_0}\right)^{\beta}\right] \quad (2)$$

where T_f is the (fictive) temperature at which a glass is in internal equilibrium, i.e., its properties are the same as that of the equilibrium liquid, A is a parameter equal to τ_0 when both T and T_f are formally infinite, x is the non-linearity parameter, Δh^* the activation energy, ϕ is the relaxation function, and β the relaxation time distribution parameter. In this formalism, x and β have values between 0 and 1, τ_0 depends upon the structure and hence on T_f. The enthalpy against T plots modeled for the quenched and slowly precooled (or annealed) samples show points of inflexion, which appear at the same T at which the peak and minimum appear in the plots of $(-dH_m/dt)$ against T. For instructive purpose, an illustration of such plots for heating of rapidly precooled and slowly precooled samples is provided in Fig. 3A. At the point of inflexion at T_1 for a rapidly precooled sample, $(-dH_m/dt)$ would show an exothermic peak and at the point of inflexion at T_2 for the slowly precooled sample, $(-dH_m/dt)$ would show a minimum. The illustration is similar to that provided by Oguni et al. in Fig. 1(a) of Ref. [2] and in Fig. 1(b) of Ref. [20]. It will be contrasted against the high temperature $(-dH_m/dt)$ feature in Fig. 1 here in Section 7.

4. Dependence of confined water's properties on pore matrix and pore size

Before interpreting the $(-dH_m/dt)$ and $C_{p,m}$ features of water in MCM-41, we note that the properties of a nanoconfined liquid depend upon the pore size, surface interactions, the number of hydrogen bonds and the bond strength. Its liquid/crystal equilibrium depends upon the commensurability between the crystal symmetry and the surface structure, upon the relative enthalpy of transformation to competing phases, and upon the Lindemann's vibration amplitude criteria for melting. Therefore, the structure of nanoconfined water and its liquid/crystal equilibrium differ from those of an identical nano-size sample inside the volume of bulk water. Moreover, water in nanopores forms a one- or two-molecules thick layer that is bonded to the silica wall. Water in this layer does not crystallize even when the remaining water in a nanopore has crystallized on cooling to ∼100 K. (It is noteworthy that existence of a liquid-like layer on the surface of ice at $T < 273$ K has been known for nearly a century, and precise atomic force microscopy has shown that surface melting of bulk ice occurs at $T > 238$ K, with the liquid-like layer thickness of ∼32 nm at ∼272 K and ∼11 nm at 263 K [60].) As self-diffusion becomes restricted in nanoconfinement, and loses its Brownian randomness, its liquid/crystal equilibrium may further differ from that in bulk water.

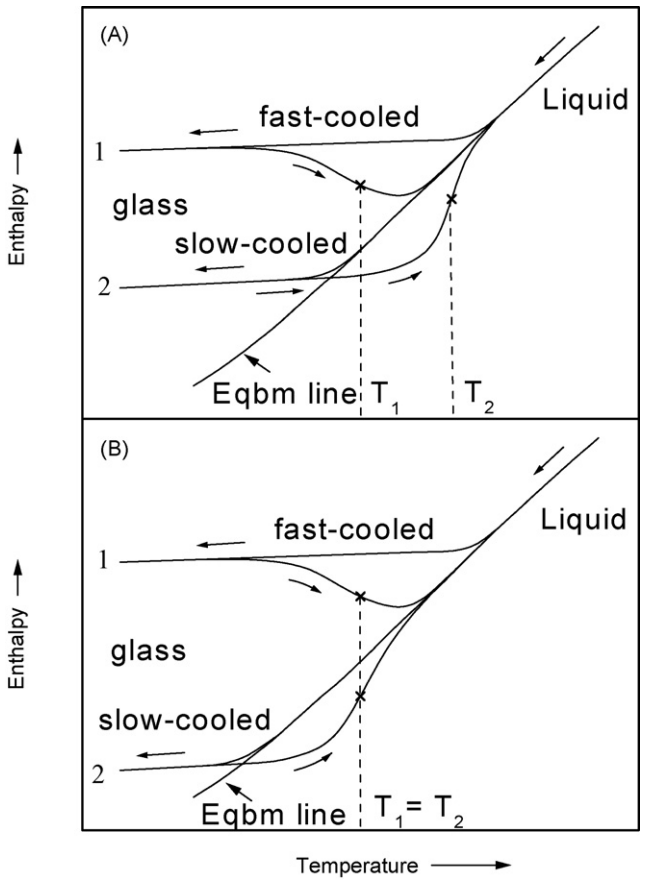

Fig. 3. (A) An illustration of the enthalpy change with T shown for a rapidly precooled sample (curve 1) and a slowly precooled sample (curve 2), drawn after Oguni et al.'s in Fig. 1(a) in [2], and Fig. 1b) in [20]. The point of inflexion T_1 is the temperature at which exothermic $(-dH_m/dt)$ peak appears on heating, and the point of inflexion T_2 is the temperature at which endothermic $(-dH_m/dt)$ minimum appears on heating, as illustrated by Oguni et al. in Fig. 1(b) [2] and Fig. 1(c) in [20]. A characteristic of kinetic unfreezing or glass-softening is that T_1 be less than T_2. (B) For instructive purposes, an illustration of the enthalpy change with T that corresponds to the data in the 180–230 K range in Fig. 1 is shown. The point of inflexion T_1 at which the exothermic $(-dH_m/dt)$ peak of a rapidly precooled sample appears, is the same as the point of inflexion T_2 at which the endothermic $(-dH_m/dt)$ minimum of slowly precooled sample appears, as in Fig. 1. Here, $T_1 = T_2$, which does not meet the requirement for kinetic unfreezing. The equilibrium liquid line is also illustrated in both panels.

Water in larger pores of silica gels, Vycor, MCM-41 and other solids has been found to crystallize over a broad temperature range at T far below 273 K, showing a freezing/melting hysteresis depending on the pore size and pore matrix [8,9,15,16,19,20], and there is an ice–water equilibrium in some pores [15,29]. In Vycor's ~4 nm size pores, water crystallizes incompletely even when cooled to 240 K at the slow rate of 6 K/h [9]. The temperature range becomes wider in smaller size pores and the enthalpy of freezing decreases when the pore size is decreased [15]. Recent DSC measurements have shown that the melting/freezing hysteresis vanishes for pore size smaller than 2.8 nm, and the enthalpy of melting cannot be detected, thus suggesting that the 2.8 nm pore size is the lowest limit for which first-order freezing/melting can be detected [16]. This conflicts with the finding from DSC, to be discussed later here that freezing occurs in 1.8 nm pores. The conflict can arise from different cooling and heating rates used in different studies.

It has been found that the energy of an H_2O molecule in Vycor's 4 nm pores varies with its position in the pore [18] and $C_{p,m}$ for water in incompletely filled pores is high, and decreases as the pores are filled [9,17]. In contrast, the enthalpy is low in incompletely filled pores, and increases as the pores are filled [17,19]. Both $C_{p,m}$ and enthalpy approach the bulk water values when the pores are filled [9,17,18]. Thus the freezing/melting features and molecular dynamics in nanoconfinement vary also with the amount of water in a given size pore. They also depend upon the technique used for studying the same sample and the cooling/heating rates, as differences have been found between the features observed by DSC and by NMR [16]. Since this difference is found to increase with decrease in the pore size [16], it would be more for water in 1.8 nm pores than in say 2.5 nm pores.

Neutron and X-ray diffraction studies have determined that nanoconfined water freezes to cubic ice with or without the growth- and stacking-faults, hexagonal ice or their mixtures [13,25,28,29,32,34,35,37–39], and in some cases to a state referred to as defective ice [28,32,34,35,37,39], containing growth- and stacking-faults [34,35], depending upon the pore size. Cubic ice forms on freezing of water in 3 nm and larger size pores. It has been found to transform irreversibly to hexagonal ice on heating. In contrast, studies of bulk state have shown that, (i) cubic and hexagonal ices coexist at equilibrium [61], (ii) water freezes directly to cubic ice [62], (iii) nano-size droplets of water can coexist with cubic ice at T in the 150–180 K range [63], and (iv) water remains at equilibrium with small ice grains in polycrystalline ice at $T < 273$ K, and both the equilibrium temperature and the fraction of water at equilibrium vary with the grain-size [64,65]. These energetically distinct processes are more easily observed by calorimetry than by NMR and diffraction techniques.

5. The low temperature enthalpy feature

In the $(-dH_m/dt)$ plots over the 90–130 K range in Fig. 1, the exothermic peak appears at a higher T than the endothermic minimum, thus clearly showing feature (I) for the t-, and T-dependent kinetic unfreezing described in Section 3. (There is weak evidence for feature (II), i.e., a small minimum at ~123 K after the exotherm, but there is no indication of a small peak after the endothermic minimum.) A prominent peak and minimum, that are similar to those in Fig. 1, were also found in the same T-range in the $(-dH_m/dt)$ plots against T for water in the 1.1 nm pores of silica gel [20] and also in the 1.2 nm and 1.6 nm pores of MCM-41 [2]. These features were attributed to the onset of diffusion of interfacial H_2O at T_g of 115 K [2].

There are difficulties in accepting that self-diffusion occurs in an uncrystallizable, one-molecule thick layer of H_2O forming a nanoshell bonded to the silica wall. To elaborate, interfacial H_2O molecules are strongly bonded to the silanol's OH group and/or to the oxygen of SiO_2, and therefore they would not contribute to structural fluctuations by Brownian motions. Moreover, it would require higher energy to free an H_2O molecule bonded to the pore wall than to free an H_2O molecule in bulk water before it can diffuse. Therefore, as the probability of self-diffusion is less in interfacial water than in bulk water, kinetic unfreezing temperature of interfacial water would be higher than that of bulk water, i.e., the relaxation time of bulk water at interfacial water's T_g of 115 K [2] would be much shorter than 1 ks. But the relaxation time for bulk water at 115 K, as extrapolated over 21 K range from its value of 10–30 s [66,67] at T_g of ~136 K [50] is much longer than 1 ks when either the Vogel–Fulcher–Tamman or the Arrhenius equation is used with a reasonable value of activation energy.

We now consider the state of H_2O in the nanoshell, i.e., at the SiO_2 interface. Neutron scattering and NMR studies [37] have shown that, in addition to the hexagonal and cubic ices in nanopores, a disordered ice/water component is present down to 200 K or lower T and a rotationally mobile state of "plastic ice" of maximum thickness of 1–1.5 nm is present at the SiO_2 surface [37]. As noted earlier here, $(-dH_m/dt)$ features similar to those in the 90–130 K

range in Fig. 2 have been observed for rotationally mobile crystals, and the more relevant hexagonal and cubic ices and ice clathrates [51–53]. In the latter, the feature has provided not only the onset temperature of rotational unfreezing of H_2O molecules but also the consequent gain in the entropy. The $(-dH_m/dt)$ feature is very small for the ices and substantial for the ice clathrates, because the number of energetically distinguished configurations in the tetrahedrally hydrogen-bonded structure of ice clathrates is more than that in the ices. Since a crystal-like order is not required for observing the $(-dH_m/dt)$ feature, H_2O molecules anchored to the pore wall would show these features. Also, as no two H_2O have the same environment, energy or near-neighbor distances [68] in the nanoshell, the number of energetically distinct configurations available to its structure would be much greater than that available to the structure of ice clathrates. Consequently, the $(-dH_m/dt)$ features arising from rotational unfreezing of H_2O bonded to the silica wall would be relatively more prominent. Accordingly, we attribute the $(-dH_m/dt)$ features in the 90–130 K range to the onset of rotational freedom in the nanoshell H_2O.

These $(-dH_m/dt)$ features would depend upon at least four effects, (i) variation of the local (interfacial) strain arising from a difference between the thermal expansion coefficients of the nanoshell and the silica wall with T, (ii) variation in the strength of hydrogen bonds between the nanoshell and the nanocore H_2O with T, (iii) variation of the enthalpy and of $C_{p,m}$ with the amount of water in the pores [9,17] and (iv) variation in the energy of an H_2O molecule with its position in a pore [18]. These competing effects would cause the $(-dH_m/dt)$ features to change with the pore size in an unsystematic manner, as is evident in Oguni et al.'s [2] study of water in MCM-41 pores. Briefly, their data in Fig. 3 [2] show that the $(-dH_m/dt)$ peak height first decreases from 0.65 mJ/(s mol) for water in 1.8 nm pores to 0.40 mJ/(s mol) for water in 1.6 nm pores, and then increases to 0.65 mJ/(s mol) for water in 1.2 nm pores. The depth of the endothermic $(-dH_m/dt)$ minimum also decreases similarly and then increases.

6. The medium temperature enthalpy feature

The relatively small $(-dH_m/dt)$ feature in the 128–170 K range also shows the required characteristic of kinetic unfreezing, i.e., the peak appears at a lower T than the minimum. Strictly speaking, it means that there is another configurational fluctuations that occurs over a well-separated and slower time scale. Since its origin has not been given [2], we consider it here: Karyakin et al.'s [69] have shown that the hydrogen bond between H_2O and –Si–OH is about 2–2.5 times more stable than the hydrogen bond between two H_2O molecules and, therefore, –Si–OH group is a better proton donor than H_2O, this feature would not arise from self-diffusion of H_2O in the nanoshell (interfacial) water strongly hydrogen bonded to the OH group of –SiOH and/or to the oxygen of SiO_2. (They also argued [69] that the O atom of SiO_2 forms a strong hydrogen bond with H_2O and as a result, the silica surface has a strong polar character and consequently holds H_2O at the interface even at high temperatures. The strength of these bonds and their chemical equilibrium at the surface is evident from the fact that surface water is only incompletely lost when SiO_2 is heated to ~473 K, as in the drying of the usual silica gel, and some of it is quickly regained on cooling in a humid atmosphere.) Such hydrogen bonds have been illustrated by Grünberg [45] in relevance to NMR studies.

Therefore, there would be two chemical equilibria in the water's nanoshell in MCM-41 pores, (1) $–Si–OH + H_2O \leftrightarrow –Si–OH\cdots O(H)_2$, i.e., hydrogen bonding between the H of silanol and O of H_2O, or O of silanol and H of H_2O and (2) $–Si–O + H_2O \leftrightarrow –Si–O\cdots H–O–H$, i.e., hydrogen bonding between O of SiO_2 and H of H_2O. Among these two, (1) is seen to be dominant because the population of –Si–OH is greater than that of –Si–O. The $(-dH_m/dt)$ feature would then be due to the t- and T-dependent equilibrium constant for reaction (1), which may be described in terms of the change in the number of hydrogen bonds, n_{bond} with T. Since H-bonding is exothermic, n_{bond} would increase on cooling and, after a certain T determined by the cooling rate has been reached, n_{bond} would not increase on further cooling. As the chemical equilibrium becomes frozen-in, n_{bond} would remain less than its equilibrium value. On heating thereafter, n_{bond} would approach the equilibrium value in a t- and T-dependent manner. This would produce the exothermic $(-dH_m/dt)$ peak for a slowly precooled sample at a certain T and a minimum for a rapidly precooled sample at a higher T. Such an equilibrium can be mathematical described in terms of a two-site model based upon Schottky's description [70], for which the modeled plots of the enthalpy and $C_{p,m}$ against T resemble the features of kinetic unfreezing or glass-softening [71–73]. Since the hydrogen bond in (1) is stronger than the hydrogen bond between two H_2Os, its $(-dH_m/dt)$ feature would appear at a higher T than the $(-dH_m/dt)$ feature due to unfreezing of orientational motion of H_2O anchored to the pore wall, even if the orientational motion required breaking of hydrogen bonds with other H_2Os.

To test the merits of this interpretation, we recall that the surface to volume ratio increases when the pore size is decreased. Therefore, fractional population of H_2O on the pore surface would increase with decreasing pore size. Accordingly, the strength of the $(-dH_m/dt)$ feature would be less when H_2O is confined to larger pores than when confined to smaller pores. In Fig. 3 of Ref. [2], we find that the $(-dH_m/dt)$ peak height in the 128–170 K range is 0.07 mJ/(s mol) for water in 1.8 nm pore, 0.21 mJ/(s mol) for water in 1.6 nm pore size, and 0.94 mJ/(s mol) for water in 1.2 nm pore. A similarly large change occurs for the $(-dH_m/dt)$ minimum. This seems to confirm our interpretation. (Note that increase in the strength of $(-dH_m/dt)$ feature with decrease in the pore size would be inconsistent with kinetic unfreezing of the nanocore H_2O molecules, because the nanocore volume decreases with decrease in the pore size.)

7. The high temperature enthalpy feature

At first sight, the $(-dH_m/dt)$ peak and minimum in the 180–230 K range in Fig. 2 appear to indicate kinetic unfreezing or glass-softening feature, and Oguni et al. [2] accordingly suggested that T_g of both pore water and bulk water is ~210 K. Viscosity of nanoconfined water is not known, but it would be accordingly expected as $10^{13.6}$ Poise at ~210 K. But a closer look at Fig. 2 shows that the exothermic $(-dH_m/dt)$ peak appears at the *same* T of ~210 K as the endothermic $(-dH_m/dt)$ minimum. This is contrary to characteristic (I) of kinetic unfreezing or glass-softening stated in Section 3, namely, that the $(-dH_m/dt)$ peak for rapidly precooled state appear at a lower T than the $(-dH_m/dt)$ minimum for the slowly precooled state. Clearly, this feature is *inconsistent* with kinetic unfreezing. The proposed T_g of ~210 K for water [2], therefore, is questionable.

To express the $(-dH_m/dt)$ features in the 180–230 K range in Fig. 2 in terms of the enthalpy against T plots deduced usually from DSC scans, we provide an illustration in Fig. 3B. The plots have been purposely sketched such that the temperatures for the points of inflexion marked as "×" are the same in the two enthalpy curves, i.e., the $(-dH_m/dt)$ peak for the rapidly precooled sample is made to appear at the same T as the $(-dH_m/dt)$ minimum for the slowly precooled sample. Plots such as those in Fig. 3B have never been observed and cannot be generated by using Eqs. (1) and (2). (In contrast, the corresponding points of inflexion appear generally at different temperatures, T_1 and T_2, as in Fig. 3A.)

For further scrutiny, we generated the enthalpy against T plots by using several sets of the A, Δh^*, β and x parameters in Eqs. (1) and

(2), and found that no combination of the parameters with $0 < \beta < 1$ and $0 < x < 1$ could produce plots resembling curves 1 and 2 in Fig. 3B, or else the $(-dH_m/dt)$ peak at the same T as the minimum. Nevertheless, the difference between the peak and minimum temperatures in the 180–230 K range decreased to ∼2 K for $\beta = 2$ and $x = 1$. We conclude that the $(-dH_m/dt)$ feature in the 180–230 K cannot be described by a nonexponential, nonlinear relaxation. Therefore, we need to search for its origin in the liquid/crystal equilibrium.

Crystallization requires homogeneous and/or heterogeneous nucleation. Briefly, the growth rate of a critical size nucleus in a liquid is equal to its decay rate, and only those molecular clusters that fluctuate to a larger size grow; nucleation rate is defined as the number of clusters per unit time that grow larger than the critical size and nucleation and growth occur at random sites. For crystallization to occur, it is crucial that the volume of liquid contain sufficient molecules to form a critical size nucleus, an aspect overlooked in discussion of nanoconfined liquids. To consider whether nucleation can occur in 1.8 nm pores of MCM-41, we note that a water molecule has an average volume of ∼30 Å^3 (=18/6.03 × 10^{23}). The effective diameter of its circumscribed sphere is therefore 0.385 nm. If the H_2O nanoshell were one-molecule thick, there will be three H_2O molecules (=(1.8/0.385) − 2) left to form a nanocore of ∼1 nm diameter in a 1.8 nm diameter pore. If it were two-molecules thick, there will be only one H_2O molecule (=(1.8/0.385) − 4) left to form the nanocore of ∼0.3 nm diameter. It has been estimated that there are 350 H_2O molecules in a critical size nucleus formed on a substrate at 231 K, and more at higher T [74]. Since homogeneous nucleation would produce a critical size nucleus containing at least a comparable number of molecules, nucleation would not occur in the water confined to 1.8 nm pores. This means that in nanopores, (a) water's crystallization does not follow the "nose-shaped", time–temperature-transformation curve, and (b) the water–ice equilibrium persists in nanopores even at low T.

For further comparison, we recall that the unit cell dimensions of hexagonal ice (space group $P6_3/mmc$, containing four H_2O) are, $a = b = 0.448$ nm and $c = 0.731$ nm, and of cubic ice (space group = $\bar{4}3m$, containing eight H_2O) are, $a = 0.638$ nm. The 1 nm diameter nanocore is slightly wider and the 0.3 nm diameter core much narrower than these unit cells. Clearly several unit cells would not form in the above-given nanocore diameter. Alternatively, a sphere of ∼1 nm diameter has a volume of 524 Å^3 (=$5^3 \times 4\pi/3$). It would contain ∼17 (=524/30) H_2O molecules, which are insufficient for forming enough unit cells of ice to produce Bragg peaks at large angles. Bragg peaks observed at low angles themselves would be broadened due partly to distortion of the unit cells and partly to small crystal size. In some cases, this may be confused as diffraction from a disordered structure.

It is conceivable that critical size nuclei form in the (excess) water outside the pores and grow into the pore water. This growth would also be limited to the extent of few distorted unit cell width of hexagonal or cubic ice because the 1 nm cross-section of nanocore cannot contain more unit cells. It is believed that the density of water on supercooling approaches the density of ice at $T < 225$ K (see also discussion in [8]). This may not be the case in structurally different water in nanopores. However, if the volume increase on crystallization was the same as for bulk water it would produce a maximum of ∼2 kbar pressure in a hermetically sealed pore at 250 K, or else expel some of the water from the pore that is open or loosely plugged at one end. In the latter case, the expulsion rate of water would determine the growth rate of ice in the sample. The ice-like structure formed along the pore axis would remain exceptionally small even if pressure persisted in the pore.

It is known that in bulk polycrystalline ice, water and ice micro-grains remain at thermodynamic equilibrium over a wide temperature range [64,65]. This occurs when a change in the interfacial energy at the grain junctions and grain boundaries becomes equal to the opposite change in the Gibbs energy per unit volume [64]. When a microcrystalline ice is cooled, ice grains grow at the expense of water at grain junctions and grain boundaries, which shrink. When it is heated, the volume of water in grain junctions and grain boundaries increases at the expense of the ice grains, which shrink. Thus crystallization and melting occur gradually over a wide temperature range. Maximum crystallization occurs only on cooling to a low T and, even at that low T, an uncrystallizably small number of H_2O molecules persist in grain junctions and grain boundaries. It bears a similarity with the gradual crystallization of the water confined to 4 nm size pores in Vycor for which the $C_{p,m}$ value of hexagonal or cubic ice was not reached even after ∼6 h of cooling from 270 K to 233 K at 6 K/h rate. (For self-diffusion coefficient of 10^{-6} cm^2/s for bulk water at 234 K [75], crystallization is expected to be rapid but that is not the case for water in 4 nm pores.) NMR studies [4,42,43] have shown similarly small correlation times for water in 1.4–2.4 nm pores in MCM-41 and neutron scattering data have yielded similarly small average translational relaxation time [4,13,30,42], and yet crystallization in these pores is slow and the "melt" coexist with ice-like structures. Melting was also gradual in Vycor's 4 nm pores. It began at a lower T than freezing and was completed over a temperature range of 15 K when the sample was heated at 6 K/h rate [9], thus showing a significant hysteresis relative to freezing. NMR cryoporometry studies have shown a hysteresis between the freezing and melting curves that varied with the surface to volume ratio and the curvature of the pore surface [76], and slow crystallization and melting have been found in 1.8 nm pores of MCM-41 (to be published). X-ray diffraction studies of water in 3.5 nm pores have shown a continuous transition between the liquid and crystalline state that precedes the first order freezing transition of pore water [8].

In summary, (i) crystallization of water in nanopores occurs over a wide T-range on cooling, as does "melting" of the crystals on heating, (ii) a thermodynamic equilibrium between the melt and ice-like structures including the growth- and stacking-faults is maintained over a wide T-range, as occurs in fine-grained ice, and it may include H_2O in the nanoshell. One expects that the difference between the energies of the "melt" and such structures [28,32,34,35,37,39] would be less than the difference between the energies of bulk water and ice. This would extend the temperature range of the equilibrium in nanopores. DSC studies by Liu et al. [77] have shown a melting endotherm at ∼212 K when precooled water in 1.8 nm pores of MCM-41 was heated. (In Fig. 2 caption, they state [77], "freezing temperature" from the "sharp negative-going peaks" but in the text, "melting points" from "inverted peaks". These inverted or negative-going peaks represent endotherms and therefore they indicate melting.)

We propose that ice-like structures with growth- and stacking-faults grow at a progressively slower rate when water in 1.8 nm pores is cooled, and "melt" on heating at a progressively faster rate. When a certain T is reached on cooling, the growth becomes too slow and ceases to occur on an experiment's time scale and further cooling does not lead to further growth. A rapidly precooled sample to 80 K would therefore contain less of the ice-like structure (and growth-and stacking-faults) than a slowly precooled sample. Both samples approach equilibrium on heating at a t- and T-dependent rate. A rapidly precooled sample approaches equilibrium by further growth of such structures and an exothermic $(-dH_m/dt)$ peak appears, and the slowly precooled sample approaches equilibrium by "melting" of the structures, and an endothermic $(-dH_m/dt)$ minimum appears. In this process, configurational and vibrational contributions to thermodynamics change continuously over a broad temperature range, and there is no abrupt change characteristic of a first-order phase transition.

The above-given origin has one testable consequence: if the pore size is decreased, the nanocore diameter would decrease and there

will be less ice-like structures including the growth- and stacking-faults formed on cooling. Thus both the $(-dH_m/dt)$ peak and the $(-dH_m/dt)$ minimum will attenuate, ultimately vanishing when the pore size is smaller than the unit cells of the ices. On examining Oguni et al.'s data in their Fig. 3 [2] for smaller size nanopores, we find that the height (and strength) of the highest temperature $(-dH_m/dt)$ peak and minimum decrease from 0.8 mJ/(s mol) for water in 1.8 nm pore to 0.35 mJ/(s mol) for water in 1.6 nm pore. The peak and the minimum seem to vanish for water in 1.2 nm pore. The origin of the $(-dH_m/dt)$ feature given here seems to have merit.

8. The unusually large C_p increase and the C_p peak

In the plot shown in Fig. 2, $C_{p,m}$ increases with T to a peak value of ~125 J/(mol K) at ~215 K. It resembles the overshoot observed on heating an annealed or structurally relaxed glass to $T > T_g$ [78]. The resemblance led Oguni et al. [2] to use it for supporting their $(-dH_m/dt)$ features-based conclusion that T_g is ~210 K for both the nanopore water and bulk water. As the $(-dH_m/dt)$ feature in the 180–230 K range is found here to be *inconsistent* with kinetic unfreezing, we need to explain the unusually large increase in $C_{p,m}$ from ~33 J/(mol K) at 180 K to 125 J/(mol K) at ~215 K. For comparison, $C_{p,m}$ increases only by 1.6 J/(mol K) for bulk water at its T_g of 136 K [50], and by ~37 J/(mol K) on melting of bulk ice at 273 K [79].

According to the origin of the $(-dH_m/dt)$ feature in Section 7, the unusually large increase in $C_{p,m}$ and its peak at ~215 K would be due to absorption of latent heat on "melting" of ice-like structures over a broad temperature range. Since latent heat does not, in principle, change T of the sample, $(T_f - T_i)$ is very small in practice, and hence $C_{p,m} = \Delta E/(T_f - T_i)$ is high for a given ΔE. Similarly large increase in $C_{p,m}$ and a peak have been observed over a small premelting range of fine-grained polycrystalline ice [65], and other solids have shown a similar occurrence.

We suggest two more features of the $C_{p,m}$–T plots which can be used as a criteria for distinguishing a broad phase transformation from kinetic unfreezing or glass-softening: (i) For a material undergoing a broad phase transformation, the $C_{p,m}$–T plot obtained on heating an annealed state lies on the low temperature side of the plot obtained for the unannealed state, as found for ice and ice clathrates [52,53]. But for a material undergoing kinetic unfreezing or glass-softening, the $C_{p,m}$–T plot for the annealed state lies to the high temperature side of the plot for the unannealed state. (ii) For a material undergoing a broad phase transformation, the $C_{p,m}$–T plot obtained during slow cooling lies to the high temperature side of the plot obtained for fast cooling. But for a liquid undergoing vitrification, the $C_{p,m}$–T plot obtained during slow cooling lies to the low temperature side of the plot obtained during fast cooling. (Experimentally, a broad phase transformation begins at a higher T for slow cooling than for fast cooling, and kinetic-freezing on glass formation begins at a lower T on slow cooling than for fast cooling.) In some cases, combination of these features may produce the $C_{p,m}$–T plots for cooling and heating to partially superpose.

Finally, we do not imply that Brownian diffusion is absent in water confined to 1.8 nm pores of MCM-41, only that it would neither be long range, nor random. Rather, it would be local and guided along the length of the pore because sufficient volume is not available in a direction orthogonal to the pore length, and it would not control the rate of a phase transformation.

9. Conclusions

The nanocore volume in the 1.8 nm pores of MCM-41 is insufficient for critical size nuclei to form and grow. Only ice-like structures of a few distorted unit cells of low energy and entropy and growth- and stacking-faults may form and remain at thermodynamic equilibrium with the "melt". The structure of water is different in different pores, as is the structure of its frozen state.

Thermodynamics and kinetics of supercooled water in 1.8 nm pores differ, respectively, from those of bulk water, as do the properties of ice-like structure from those of bulk ice. This is evident simply from the fact that incorporation of water in nanopores is exothermic [17], i.e., interactions of an H_2O with the pore wall as well as with another H_2O in a nanopore are stronger than interactions of H_2O in the bulk, with the energy of a water molecule still varying with its position in the pore [17]. Therefore, nanopore water's T_g would differ from that of bulk water. It would be difficult to justify that confined water is in the glassy state in very small pores, because there are insufficient molecules to define the disorder and the structure formed cannot be contrasted against that of a crystal. In larger pores, properties of water may approach that of bulk water, but water in larger pores does not readily supercool, thus defeating the purpose of confinement.

The three features in the $(-dH_m/dt)$ against T plots observed on heating rapidly precooled and slowly precooled samples, and the unusually large increase in $C_{p,m}$, are attributable to processes that do not require long range diffusion of H_2O. Instead, (i) exotherm and endotherm in $(-dH_m/dt)$ in the 90–130 K range may arise from kinetic unfreezing of reorientational motions of H_2O molecules in the nanoshell bonded to the SiO_2 wall, (ii) those in the 128–170 K range may arise from unfreezing of the hydrogen bond equilibrium between H_2O and surface silanol groups, and (iii) those in the 180–230 K range, which are *inconsistent* with the kinetic unfreezing, arise from the time- and temperature-dependent growth and decay of the ice-like structures, including the growth- and stacking-faults, at equilibrium with the "melt water". Thus there are two time scales for the kinetics of configurational fluctuations corresponding to (i) and (ii). In view of their different origins, it does not seem possible to attribute the kinetic unfreezing of a particular fluctuation to glass-softening of water in 1.8 nanopores. Even if it could be done, its temperature would not be the same as the glass-softening temperature of 136 K for bulk water, because the structure and energy of nanoconfined water differ from those of bulk water. Also, NMR, neutron scattering and dielectric and mechanical relaxations do not probe *all* configurational fluctuations that occur in a liquid, and their relaxation time distribution differ from that observed in calorimetry, an effect ignored in a comparative analysis [80]. Therefore, T_g determined from these techniques differs from that measured by calorimetry.

Finally, the exceptionally large increase in $C_{p,m}$ and its peak at ~215 K is attributed to the absorption of latent heat as the ice-like structure (and the growth- and stacking-faults) "melt". The available data on pore size dependence of these features are consistent with this conclusion. The structure formed in the 1.8 nm pore would be similar to that of deformed, unit cells of ice with growth- and stacking-faults and not that of the bulk hexagonal or cubic ices. The latent heat of their "melting" that contributes to the unusual $C_{p,m}$ increase would be due to the loss of these structures.

Acknowledgements

I would like to thank D.P.B. Aji for his help in drawing the figures. This research was supported by a Discovery Grant from the Natural Science and Engineering Research Council of Canada.

References

[1] F. Mallamace, M. Broccio, C. Corsaro, A. Faraone, D. Majolino, V. Venuti, L. Liu, C.-Y. Mou, S.-H. Chen, Proc. Natl. Acad. Sci. 104 (2007) 424.
[2] M. Oguni, Y. Kanke, S. Namba, AIP Conf. Proc. 982 (2008) 34.
(The rate of slow cooling is given as "e.g. at 10 mK min^{-1}". Professor Oguni informed us that it is 15 mK/min, which does not affect our analysis, and that $C_{p,m}$ was essentially the same for both slowly-precooled and rapidly-precooled samples.).

[3] G.P. Johari, E. Tombari, G. Salvetti, F. Mallamace, J. Chem. Phys. 130 (2009) 126102.
[4] F. Mallamace, M. Broccio, C. Corsaro, A. Faraone, L. Liu, C.-Y. Mou, S.H. Chen, J. Phys.: Condens Matter 18 (2006) S2285.
[5] M.-C. Bellissent-Funel, Europhys. J. E. 12 (2003) 83.
[6] C. Alba-Simionesco, B. Coasne, G. Dosseh, G. Dudziak, K.E. Gubbins, R. Radhakrishnan, M. Sliwinska-Bartkowiak, J. Phys.: Condens Matter 18 (2006) R15.
[7] A. Schreiber, I. Ketelsen, G.H. Findenegg, Phys. Chem. Chem. Phys. 33 (2001) 1185.
[8] K. Morishige, K. Kawano, J. Chem. Phys. 110 (1999) 4867.
[9] E. Tombari, G. Salvetti, C. Ferrari, G.P. Johari, J. Chem. Phys. 122 (2005) 104712.
[10] M. Brun, A. Lallemand, J.-F. Quinson, C. Eyraud, Thermochim. Acta 21 (1977) 59.
[11] Y.P. Handa, M. Zakrzewski, C. Fairbridge, J. Phys. Chem. 96 (1992) 8594.
[12] J.C. van Miltenburg, J.P. van der Earden, J. Cryst. Growth 128 (1993) 1143.
[13] T. Takamuko, M. Yamagami, H. Wakita, Y. Masuda, T. Yamaguchi, J. Phys. Chem. B 101 (1997) 5730.
[14] A. Schreiber, I. Ketelsen, G.H. Findenegg, E. Hoinkis, in: P.L. Llewellyn, J. Rouguerol, F. Rodrigues-Reinosi, N.A. Seaton (Eds.), Characterization of Porous Solids (Studies in Surf. Sci. and Catalysis. Vol. 7), Elsevier, Amsterdam, 2006, pp. 17–24.
[15] S. Kittaka, S. Ishimaru, M. Kuranishi, T. Matsuda, T. Yamaguchi, Phys. Chem. Chem. Phys. 8 (2006) 3223.
[16] S. Jähnert, F. Vaca Chávez, G.E. Schaumann, A. Schreiber, M. Schönhoff, G.H. Findenegg, Phys. Chem. Chem. Phys. 10 (2008) 6039.
[17] E. Tombari, G. Salvetti, C. Ferrari, G.P. Johari, J. Chem. Phys. 123 (2005) 214706.
[18] E. Tombari, G. Salvetti, C. Ferrari, G.P. Johari, Phys. Chem. Chem. Phys. 7 (2005) 3407.
[19] S. Maruyama, K. Wakabayashi, M. Oguni, AIP Conf. Proc. 708 (2004) 675.
[20] M. Oguni, S. Maruyama, K. Wakabayashi, A. Nagoe, Chem. Asian J. 2 (2007) 514.
[21] A. Sanoudaki, B. Albela, L. Bonneviot, M. Peyrard, Eur. Phys. J. E. 17 (2005) 21.
[22] J. Banys, M. Kinka, J. Makutkevic, G. Völkel, W. Böhlmann, U. Venkatesan, M. Hartmann, A. Pöppl, Mater. Sci. Forum 514–516 (2006) 1255.
[23] D.C. Steytler, J.C. Dore, J.C. Wright, J. Phys. Chem. 87 (1983) 2458.
[24] M.C. Bellissent-Funel, J. Lal, L. Bosio, J. Chem. Phys. 98 (1993) 4246.
[25] K. Morishige, K. Nabuoka, J. Chem. Phys. 107 (1997) 6965.
[26] A.K. Soper, Mol. Phys. 106 (2008) 2053.
See Sect. 5.
[27] S. Takahara, M. Nakano, S. Kittaka, Y. Kuroda, T. Mori., H. Hamano, T. Yamaguchi, J. Phys. Chem. B 103 (1999) 5814.
[28] J. Dore, Chem. Phys. 258 (2000) 327.
[29] A. Fouzri, R. Dorbez-Sridi, M.M. Oumezzine, J. Chem. Phys. 116 (2002) 791.
[30] S. Takahara, N. Sumiyama, S. Kttaka, T. Yamguchi, M.C. Bellissent, J. Phys. Chem. B 109 (2005) 11231.
[31] D. Liu, Y. Zhang, C.-C. Chen, C.-Y. Mou, O.H. Poole, S.-H. Chen, Proc. Natl. Acad. Sci. 104 (2007) 9570.
[32] B. Webber, J.C. Dore, J. Phys.: Condens Matter 16 (2004) S5449.
[33] V. Venuti, V. Crupia, D. Majolinoa, P. Migliardoa, M.C. Bellissent-Funel, Phys. B: Condens Matter 350 (2004) E599.
[34] K. Morishige, H. Uematsu, J. Chem. Phys. 122 (2005) 044711.
[35] K. Morishige, H. Iwasaki, Langmuir 19 (2003) 2808.
[36] P. Smirnov, T. Yamaguchi, S. Kittaka, S. Takahara, Y. Kuroda, J. Phys. Chem. B 104 (2000) 5498.
[37] J.B.W. Webber, J.C. Dore, J.H. Strange, R. Anderson, B. Tohidi, J. Phys.: Condens Matter 19 (2007) 415117.
[38] J. Seyed-Yazdi, H. Farman, J.C. Dore, J.B.W. Webber, G.H. Findenegg, T. Hansen, J. Phys.: Condens Matter 20 (2008) 205108.
[39] J. Seyed-Yazdi, J.C. Dore, J.B.W. Webber, G.H. Findenegg, T. Hansen, J. Phys.: Condens Matter 20 (2008) 205107.
[40] W. Hansen, M. Stöcker, R. Schmidt, J. Phys. Chem. 100 (1996) 2195.
[41] F. Mansour, R.M. Dimeo, H. Peemoeller, Phys. Rev. E 66 (2002) 041307.
[42] S.H. Chen, F. Mallamace, C.-Y. Mou, M. Broccio, C. Corsaro, A. Faraone, L. Liu, Proc. Natl. Acad. Sci. U.S.A. 103 (2006) 12974.
[43] D.W. Hwang, C.-C. Chu, A.K. Sinha, L.-P. Hwang, J. Chem. Phys. 126 (2007) 044702.
[44] A. Vyalikh, Th. Emmler, B. Grünberg, Y. Xu, I. Shenderovich, G.H. Findenegg, H.-H. Limbach, G. Buntkowsky, Ziet. Fur Physikalische Chemie 221 (2007) 155.
[45] B. Grünberg, T. Emmler, E. Gedat, I. Shendorovich, G.H. Findenberg, H.H. Limbach, G. Buntkowsky, Chem. Eur. J. 10 (2004) 5689.
[46] S. Stapf, R. Kimmich, J. Chem. Phys. 103 (1995) 2247.
[47] J. Rault, R. Neffati, P. Judeinstein, Eur. Phys. J. B. 36 (2003) 627.
[48] MCM or Micelle-templated silica materials, is a series of synthesized mesoporous silica materials with unidimensional (columner) hexagonal arrangement of cylindrical pores, a narrow pore-size distribution and no pore junctions.
[49] G.P. Johari, J. Chem. Phys. 112 (2000) 8958.
See Fig. 3, and the relevant description.
[50] G.P. Johari, A. Hallbrucker, E. Mayer, Nature 330 (1987) 552.
[51] O. Yamamuro, O. Oguni, T. Matsuo, H. Suga, J. Phys. Chem. Solids 48 (1987) 935.
Instead of slow-cooling, the bulk sample in their studies had been isothermally annealed prior to heating. Both slow cooling and annealing lead to a more equilibrated state of lower enthalpy, entropy and fictive temperature, T_f.
[52] G.P. Johari, Chem. Phys. 258 (2000) 277.
[53] O. Yamamuro, M. Oguni, T. Matsuo, H. Suga, J. Phys. Chem. Solids 49 (1988) 425.
[54] H. Suga, J. Phys.: Condens Matter 15 (2003) S775.
Fig. 4 of this review provides an illustration of the dH_m/dt feature.
[55] H. Fujimori, M. Oguni, J. Chem. Thermodyn. 26 (1994) 367.
[56] H. Fujimori, M. Muzikami, M. Oguni, J. Non-Cryst. Solids 204 (1996) 38.
[57] A.Q. Tool, J. Am. Ceram. Soc. 29 (1946) 240.
[58] O.S. Narayanaswamy, J. Am. Ceram. Soc. 54 (1971) 491.
[59] C.T. Moynihan, P.B. Macedo, C.J. Montrose, P.K. Gupta, M.A. Debolt, J.F. Dill, B.E. Dom, P.W. Drake, A.J. Easteal, P.B. Eltermann, R.A. Moeller, H. Sasabe, J.A. Wilder, Ann. N.Y. Acad. Sci. 279 (1976) 15.
[60] A. Döppenschmidt, H.-J. Butt, Langmuir 16 (2000) 6709.
[61] G.P. Johari, Philos. Mag. B 78 (1998) 375.
[62] G.P. Johari, J. Chem. Phys. 122 (2005) 194504.
[63] G.P. Johari, J. Chem. Phys. 109 (1998) 1070.
[64] G.P. Johari, W. Pascheto, S.J. Jones, J. Chem. Phys. 100 (1994) 4548.
[65] G. Salvetti, E. Tombari, G.P. Johari, J. Chem. Phys. 102 (1995) 4987.
[66] G.P. Johari, Phys. Chem. Chem. Phys 7 (2005) 1091.
[67] G.P. Johari, J. Chem. Phys. 122 (2005) 144508.
[68] The entropy of a tetrahedrally hydrogen-bonded structure varies with the number of energetically distinct orientations of H_2O molecules within the constrains of hydrogen bonds, without self-diffusion or significant displacement of the molecular center of mass. When all intermolecular distances are the same, i.e., the hydrogen bond lengths are the same, as in an ideal lattice of hexagonal and cubic ices, and the six orientations of H_2O at the lattice sites have the same energy. When the intermolecular distances vary, as in high-pressure ices, ice clathrates and in imperfect lattices of all ices, the energy of the six orientations of a H_2O molecule depend upon the orientation. This increases the number of configurations accessible to the structure and leads to a t- and T-dependent configurational entropy, as for liquids. Its kinetic freezing and unfreezing produce glass-like relaxation features, stronger for ice clathrates than for hexagonal and cubic ices.
[69] A.V. Karyakin, G.A. Muradova, G.V. Maisuradze, J. Appl. Spectrosc. 12 (1970) 675 (Translation from, Zhur. Prikla. Spektros. 12 (1970) 903).
They concluded that the hydrogen bond between H_2O and SiOH is 2–2.5 times more stable than with another H_2O, and therefore the Si–OH group is a better proton donor than H_2O.
[70] W. Schottky, Phys. Z. 22 (1921) 1.
[71] P.B. Macedo, W. Capps, T.A. Litovitz, J. Chem. Phys. 44 (1966) 3357.
[72] C.A. Angell, J. Phys. Chem. 75 (1971) 3698.
[73] G.P. Johari, J. Chem. Phys. 98 (1993) 7324.
[74] J. Liu, C.E. Nicholson, S.J. Cooper, Langmuir 23 (2007) 7286.
[75] R.C. Smith, Z. Dohnalek, G.A. Kimmel, K.P. Stevenson, B.D. Kay, Chem. Phys. 258 (2000) 291.
See Fig. 8.
[76] O. Petrov, I. Furó, Phys. Rev. E. 73 (2006) 011608.
[77] L. Liu, S.-H. Chen, A. Faraone, C.-W. Yen, C.-Y. Mou, A. Mamontov, J. Leao, J. Phys.: Condens Matter 18 (2006) S2261.
[78] G.W.H. Höhne, W.F. Hemminger, H.-J. Flammersheim, Differential Scanning Calorimetry, 2nd ed., Springer, Berlin, 2003.
[79] D. Eisenberg, W. Kauzmann, The Structure and Properties of Water, Clarendon, Oxford, 1969, p. 100.
[80] G.P. Johari, D.P.B. Aji, J. Chem. Phys. 129 (2008) 056101.